

Electronic Supplementary Material

Clozapine Sensing Through Paper-based Microfluidic Sensors Directly Modified via Electro-deposition and Electro-polymerization

Mohammad Hossein Ghanbari ^{a,b}, Markus Biesalski ^b, Oliver Friedrich ^c, Bastian J.M. Etzold ^{a,b,*}

^a Friedrich-Alexander-Universität Erlangen-Nürnberg, Power-To-X Technologies; 90762 Fürth, Germany

^b Technische Universität Darmstadt, Ernst-Berl-Institute for Technical Chemistry and Macromolecular Science, Peter-Grünberg-Straße 8, 64287, Darmstadt, Germany

^c Institute of Medical Biotechnology, Department of Chemical and Biological Engineering, Friedrich-Alexander-Universität Erlangen-Nürnberg (FAU), Paul-Gordan-Str. 3, 91052, Erlangen, Germany

ORCID: Mohammad Hossein Ghanbari: 0000-0003-0951-8028, Markus Biesalski: 0000-0001-6662-0673, Oliver Friedrich: 0000-0003-2238-2049, Bastian Etzold: 0000-0001-6530-4978

✉ Bastian J.M. Etzold (bastian.etzold@fau.de)

Electrochemically active surface area

The calculated electrochemically active surface area (A) of the μCS , ED- μCS , EP- μCS , ED/EP-ser- μCS , and ED/EP-sim- μCS (Figure S1) was estimated to be 0.316 cm², 0.884 cm², 0.681 cm², 0.920 cm², and 1.140 cm², respectively. Consequently, employing the simultaneous electro-deposition of AuNPs and electro-polymerization of poly (L-cys) onto the WE surface, increases the A value and amplifies the current signal of the modified platforms.

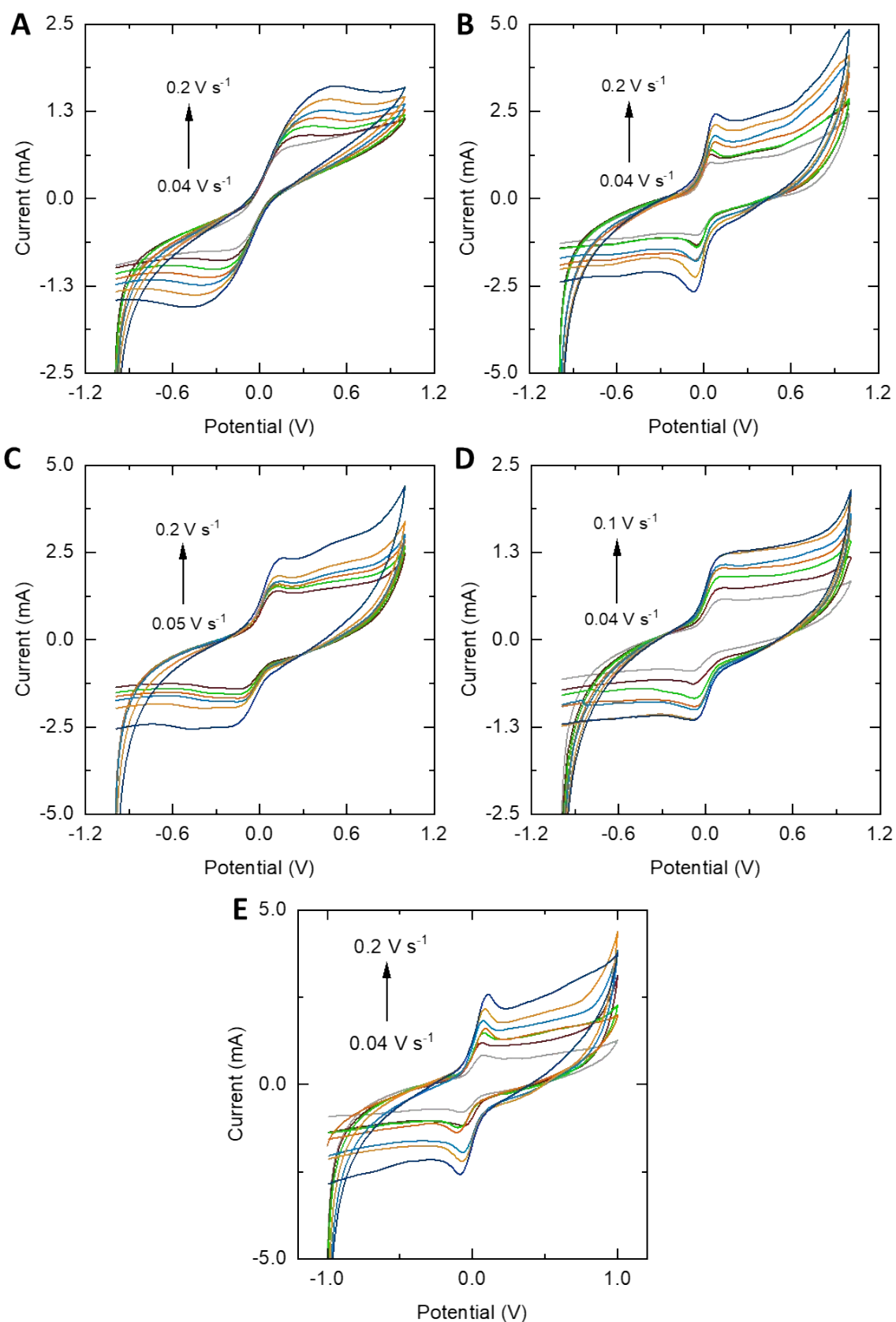


Figure S1. CVs of 5 mM of $K_3Fe(CN)_6$ in 0.1 M KCl at various scan rates on different electrodes (A) bare μCS , (B) AuNPs ED- μCS , (C) L-cys EP- μCS , (D) ED/EP-ser- μCS , and (E) ED/EP-sim- μCS .

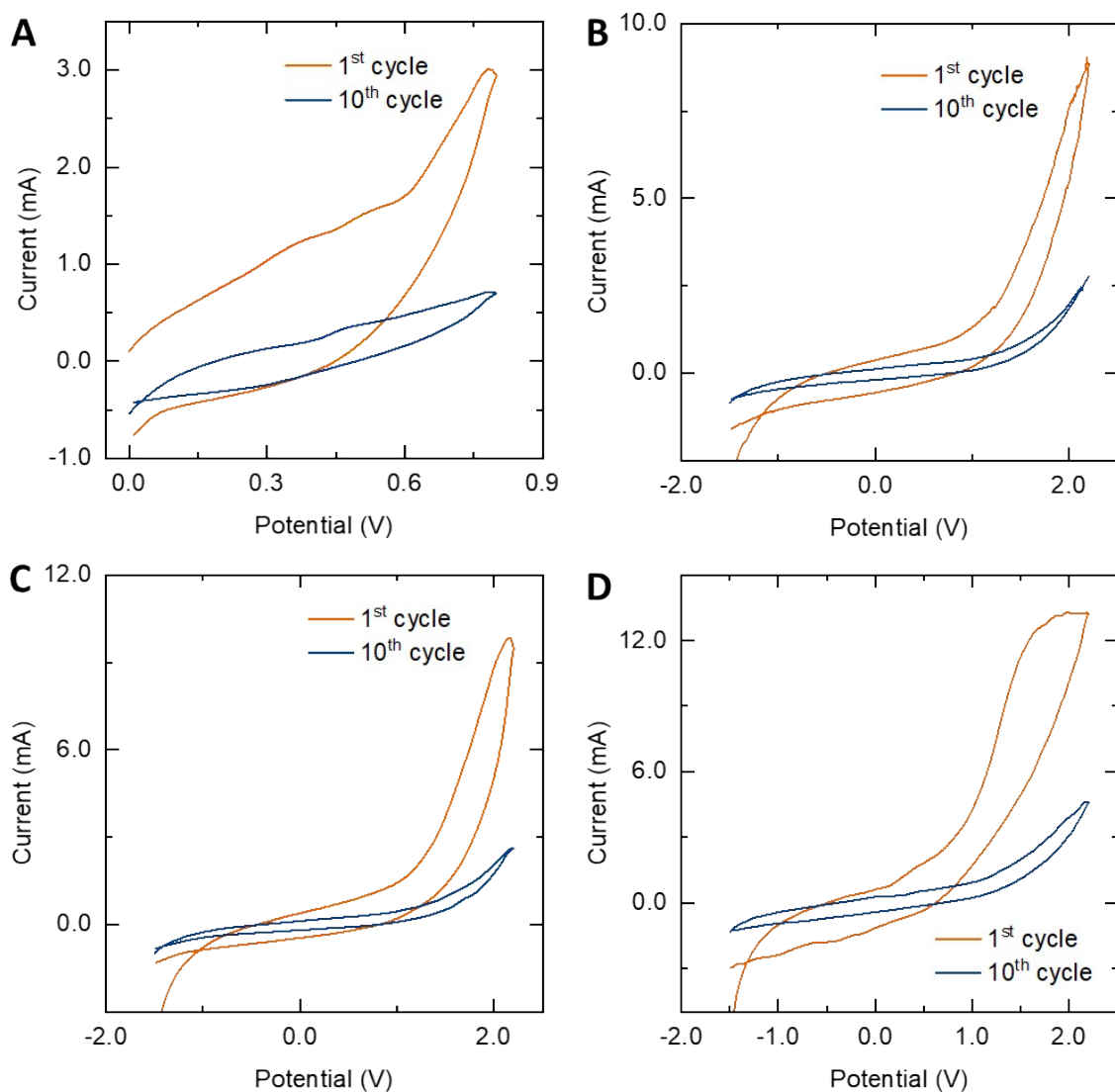


Figure S2. (A) AuNPs electro-deposition for 10 cycles onto the bare μ CS surface at 0.1 M PBS at pH=7 containing 1.0 mM HAuCl_4 and 0.1 M KNO_3 from 0.0 V to +0.8 V under a scan rate of 50 mV s^{-1} , (B) L-cys electro-polymerization for 10 cycles onto the bare μ CS at 0.1 M PBS at pH=6 containing 1.0 mM L-cys from -1.5 V to +2.2 V under a scan rate of 50 mV s^{-1} , (C) L-cys electro-polymerization onto the AuNPs ED- μ CS (first step A and then step B), and (D) simultaneous AuNPs electro-deposition and L-cys electro-polymerization for 10 cycles onto the bare μ CS surface, AuNPs/L-cys [1.0 mM : 1.0 mM], under a scan rate of 100 mV s^{-1} from -1.5 V to +2.2 V.

Table S1. A summary of the EIS parameters.

Platform	Parameter	Value	Error%
μ CS	$R_{ct}(\Omega)$	46	4.5
	$R_s(\Omega)$	28	4.2
	$R_{dl}(F)$	8.5×10^{-7}	9.5
	$Z_w(\Omega/\text{Hz}^{1/2})$	3.0×10^{-3}	4.1
ED/EP-sim- μ CS	$R_{ct}(\Omega)$	13	11.6
	$R_s(\Omega)$	16	5.1
	$R_{dl}(F)$	9.2×10^{-6}	16.5
	$Z_w(\Omega/\text{Hz}^{1/2})$	1.3×10^{-2}	7.8

Effect of the AuNPs/L-cys concentration ratio

Various concentration ratio of gold (III) chloride trihydrate/ L-cys solutions including a: gold/L-cys [0.5 mM: 1.0 mM], b: gold/L-cys [1.0 mM: 0.5 mM], and c: gold/L-cys [1.0 mM: 1.0 mM] in 0.1 M ABS at pH 6.0 were prepared. At the following step, 2 mL of these solutions were dropped onto the sponge and used for the S (ED & EP) as described in the experimental section. Then, the prepared sensors were studied under identical conditions by LSV in a redox probe solution containing 5 mM of $[\text{Fe}(\text{CN})_6]^{3-/4-}$ and 0.1 M KCl, under a scan rate of 100 mV s^{-1} (Figure S3). Also, to study the morphology of the nanostructures obtained onto the WE surface, SEM images were recorded (Figure S4). As shown in Figure S3&S4, among different concentration ratios, at the concentration ratio of [1.0 mM: 1.0 mM] gold/L-cys solution, the highest peak current was observed. Although with the concentration ratio of 0.5 mM gold: 1.0 mM L-cys, higher amount of nanocomposite was formed on the WE surface in comparison with 1.0 mM gold: 1.0 mM L-cys, the oxidation peak current decreased. Presumably, the formation of a thick film of nanocomposite leads to longer diffusion distance as well as higher ohmic resistance. The further increase in gold concentration (1.0 mM gold: 0.5 mM L-cys), caused a decrease in the peak current and, therefore, had a smaller effect in improving the current. Therefore, the optimized amount of the concentration ratio of gold/L-cys solution was chosen as [1.0 mM: 1.0 mM], and the positive effects of ED/EP-sim discussed previously can be leveraged.

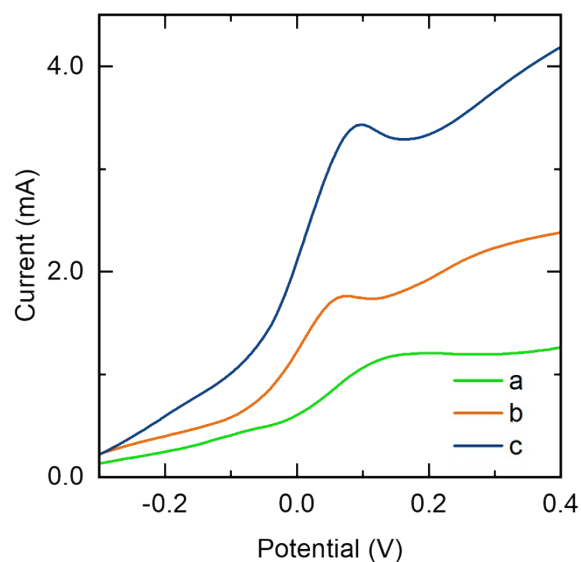


Figure S3. The recorded LSV for the proposed platform (simultaneous AuNPs electro-deposition and L-cys electro-polymerization for 10 cycles, under a scan rate of 100 mV s^{-1} from -1.5 V to +2.2 V) at the various concentration of AuNPs and L-cys in the electrode modification process (a: AuNPs/L-cys [0.5 mM : 1.0 mM], b: AuNPs/L-cys [1.0 mM : 0.5 mM], and c: AuNPs/L-cys [1.0 mM : 1.0 mM] in 0.1 M ABS at pH 6.0), in a redox probe solution containing 5 mM of $[\text{Fe}(\text{CN})_6]^{3-/4-}$ and 0.1 M KCl under a scan rate of 100 mV s^{-1} .

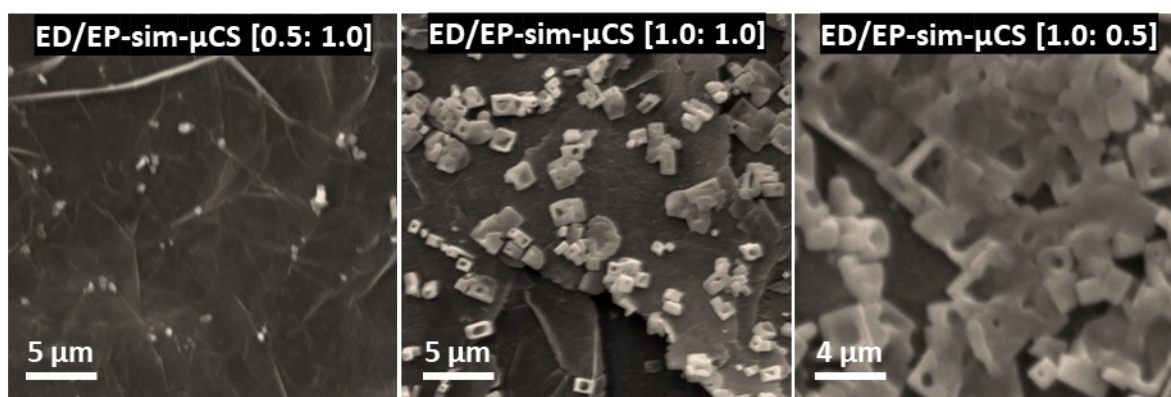


Figure S4. The recorded SEM images of the different concentration of AuNPs and L-cys in the electrode modification process.

Effect of the potential windows on the electrode modification process

In order to obtain the high sensitivity and stability required, various potential windows in the electrode modification process were studied. Briefly, three different WE, prepared using CV from -0.4V to +0.8 V, -1.5 V to +0.8 V, and -1.5 V to +2.2 V, were examined through their voltammetric signals under identical conditions and as shown in Figure S5, the best result was achieved using the potential window from -1.5 V to +2.2 V for $[\text{Fe}(\text{CN})_6]^{3-/4-}$ oxidation as a standard redox probe solution. When the potential window is wider, the signal increases, this can be due to better formation of nanocomposite onto the WE surface. Therefore, the potential window from -1.5 V to +2.2 V was chosen as the optimum potential window for formation of the modifier.

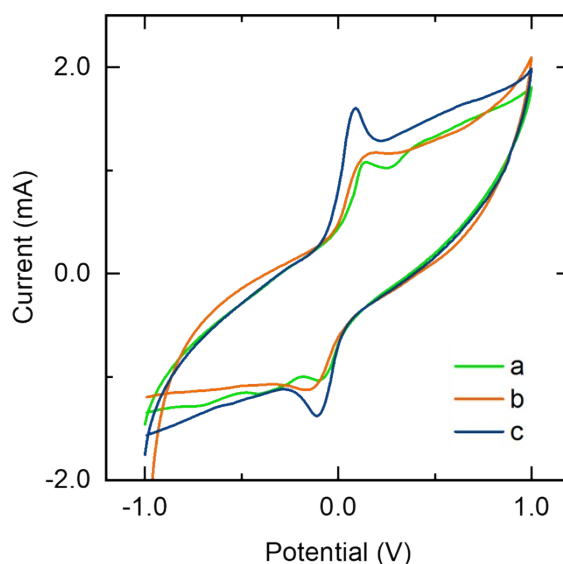


Figure S5. The recorded CV for the proposed platform (simultaneous AuNPs electro-deposition and L-cys electro-polymerization for 10 cycles, AuNPs/L-cys [1.0 mM : 1.0 mM] in 0.1 M PBS at pH 6.0, under a scan rate of 100 mV s^{-1}) at the various potential windows in electrode modification process (a: -0.4V to +0.8 V, b: -1.5 V to +0.8 V, and c: -1.5 V to +2.2 V), in a redox probe solution consisting 5 mM of $[\text{Fe}(\text{CN})_6]^{3-/4-}$ and 0.1 M KCl under a scan rate of 100 mV s^{-1} .

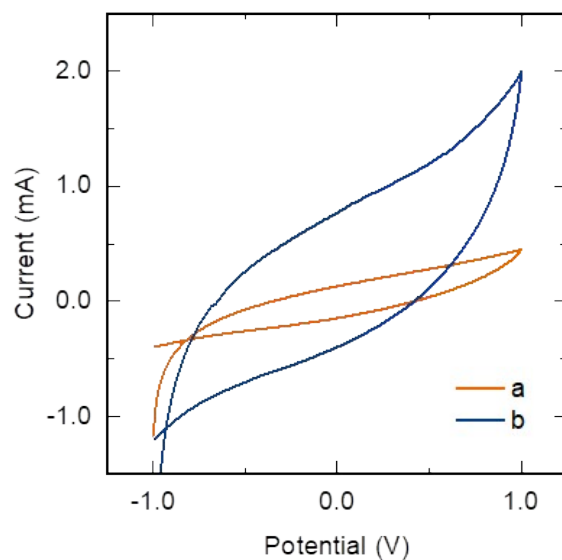


Figure S6. The recorded CV for the bare μCS (a), and proposed modified μCS (b) in 0.1 M blank PBS (pH=8.0) at scan rate of 100 mV s^{-1} .

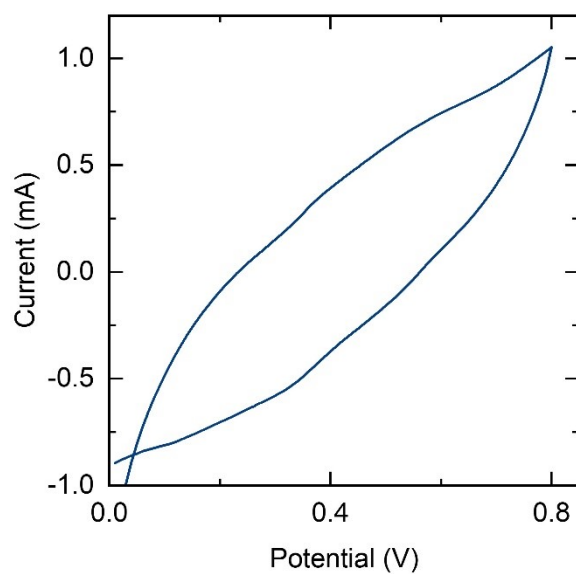


Figure S7. The recorded CV for the proposed modified μCS in a solution comprising $3.0 \mu\text{M}$ CLZ (pH=8.0) at scan rate of 100 mV s^{-1} .

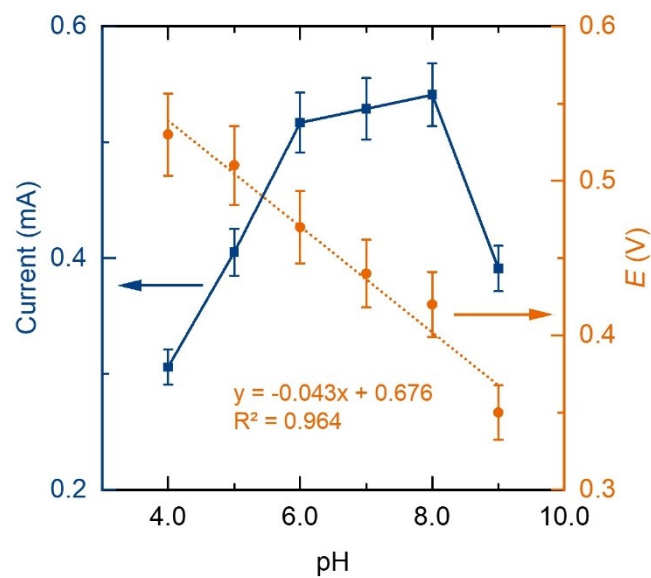


Figure S8. Effect of pH of CLZ solutions on the I_{pa} and E_{pa} in a solution comprising $3.0 \mu\text{M}$ CLZ.

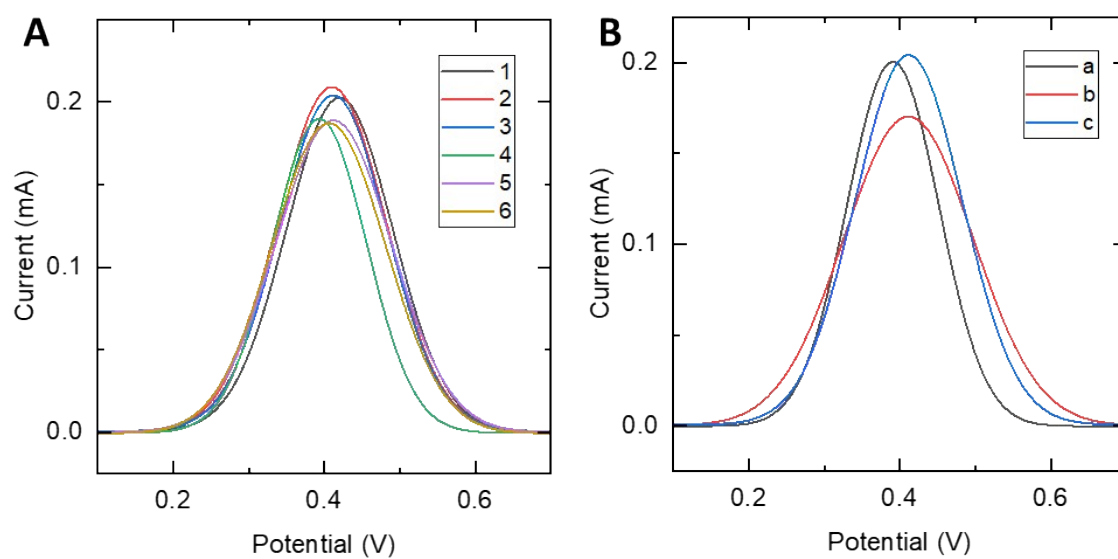


Figure S9. (A) Recorded SWVs of the ED/EP-sim- μCS for the (A) Stability and (B) Reproducibility study for the different devices under $10.0 \mu\text{M}$ of CLZ in 0.1 M PBS at $\text{pH} = 8.0$.

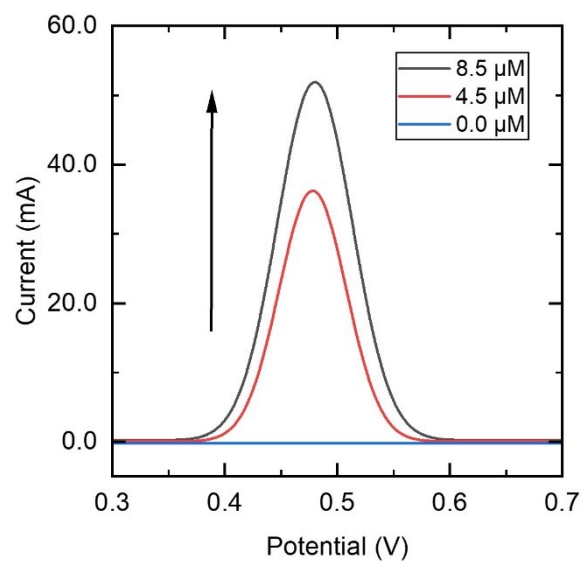


Figure S10. SWVs of the ED/EP-sim- μ CS in human blood serum sample for various concentrations of CLZ in 0.1 M PBS (pH = 8.0).